A C-3 Methylated Isocembranoid and 10-Oxocembranoids from a Formosan Soft Coral, *Sinularia grandilobata*

Atallah F. Ahmed,[†,‡] Shu-Hui Tai,[†] Zhi-Hong Wen,[†] Jui-Hsin Su,[†] Yang-Chang Wu,[§] Wan-Ping Hu,[∥] and Jyh-Horng Sheu*[,†,⊥]

Department of Marine Biotechnology and Resources, National Sun Yat-sen University, Kaohsiung 804, Taiwan, Republic of China, Department of Pharmacognosy, Faculty of Pharmacy, Mansoura University, Mansoura 35516, Egypt, Graduate Institute of Natural Products, Kaohsiung Medical University, Kaohsiung 807, Taiwan, Republic of China, Faculty of Biotechnology, Kaohsiung Medical University, Kaohsiung 807, Taiwan, Republic of China, and Asia-Pacific Ocean Research Center, National Sun Yat-sen University, Kaohsiung 804, Taiwan, Republic of China

Received December 19, 2007

Five new cembranoids, designated grandilobatins A−E (**1**−**5**), were isolated from the soft coral *Sinularia grandilobata*. Grandilobatin C (**3**) was found to have a novel skeleton with the C-4 methyl group of the normal cembranoid rearranged to C-3, while the other metabolites were identified as new 10-oxocembranoids. Metabolite **4** has weak cytotoxicity toward MDA-MB-23 human breast tumor cells. Also, **4** significantly inhibited the accumulation of the pro-inflammatory iNOS protein of LPS-stimulated RAW264.7 macrophage cells at 50 μM.

Marine terpenoids are considered as metabolites of great interest due to their unique structures and wide range of biological activities.[1] Previous chemical investigations on the Formosan soft corals of the genus *Sinularia* have afforded several cembranoids[2–6] and norcembranoids,[7–11] some of which have been shown to exhibit cytotoxic activity against the growth of various cancer cell lines.[4,8–10] Recently, our chemical examination on the Formosan soft coral *Sinularia grandilobata* Verseveldt (Alcyonacea) resulted in the isolation of four trihydroxysteroids.[12] Further investigation on the constituents of this soft coral has led to the isolation of five new cembrane-derived diterpenes, grandilobatins A−E (**1**−**5**). Among these, grandilobatin C (**3**) was characterized as a new skeletal 4,10-dioxoisocembranoid with a methyl group of the normal cembranoid rearranged from C-4 to C-3, while another five metabolites were recognized as 10-oxocembranoids. Herein, we report the isolation, structure elucidation, and biological activity of these compounds.

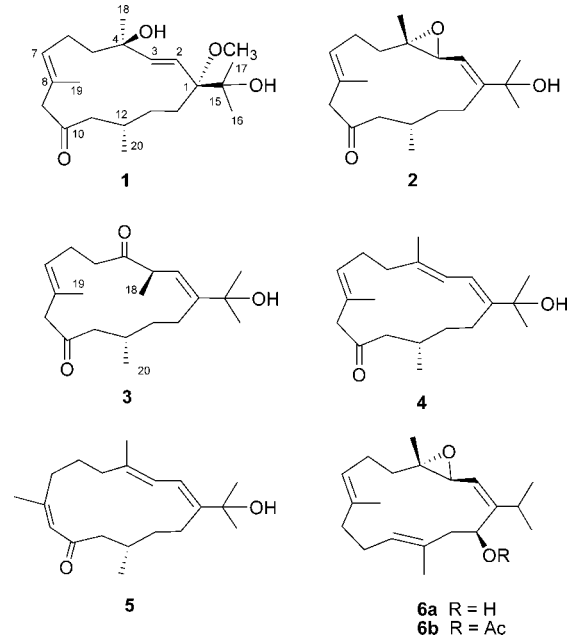

Results and Discussion

The EtOH extract of *S. grandilobata* was partitioned between CH_2Cl_2 and H_2O to afford the CH_2Cl_2-soluble fraction, which was then subjected to Si gel column chromatography. The fraction containing terpenoids was selected after the ^{1}H NMR spectrum revealed the presence of various terpenoids, and this fraction was further purified by a series of normal and reversed-phase HPLC to afford **1**−**5** (see Experimental Section).

Grandilobatin A (**1**) was obtained as the most polar metabolite. Its HRESIMS (*m*/*z* 375.2514 $[M + Na]^+$) established the molecular formula $C_{21}H_{36}O_4$, requiring four degrees of unsaturation. The IR spectrum of **1** revealed the presence of hydroxy (ν_{max} 3422 cm^{-1}), carbonyl (ν_{max} 1699 cm^{-1}), and olefinic ν_{max} 1653 cm^{-1}) moieties, and a methoxy group was recognized as being present in the molecule from the NMR signals (Tables 1 and 2) at δ_H 3.20 (3H, s) and δ_C 51.5 (CH_3). Also, the ^{1}H NMR spectrum of **1**, measured in $CDCl_3$, displayed six methyl groups (Table 1) including three tertiary methyls (δ 1.12, 6H, s and 1.39, s), one olefinic methyl (δ 1.78, 6H, s), one secondary methyl (δ 0.99, 3H, d, J = 7.0 Hz), and one methoxy methyl (δ 3.20, 3H, s). Two of the three tertiary methyls were found to be the partial structures of a hydroxyisopropyl group, and the third was found to be attached to a tertiary hydroxyl-bearing carbon, revealed by the HMBC correlations of protons of the former two methyls to the carbon signal at δ 75.8 (qC), and the latter methyl to the carbon signal at δ 73.6 (qC), respectively (Figure 1). In the lower field of the ^{1}H NMR spectrum, the proton signal appearing at δ 5.17 (1H, br dd, J = 7.0, 7.0 Hz) indicated the presence of a trisubstituted olefin. The 2H singlet at δ 5.68, measured in $CDCl_3$, was resolved by measuring the ^{1}H NMR spectrum in C_6D_6 (see Experimental Section) into two doublets (δ 5.64 and 5.76, each 1H, d, J = 16.5 Hz) attributable to a *trans* 1,2-disubstituted double bond. The^{13}C NMR spectrum of **1** showed the presence of 21 carbons (Table 2), including six methyls, one carbonyl (δ 208.5, qC), two olefinic double bonds (δ 140.8, CH, 130.4, qC, 129.1, CH, and 128.1, CH), six sp^3 methylenes, one sp^3 methine, and three oxygen-bearing quaternary carbons. By the analysis of ^{1}H−^{1}H COSY correlations, it was possible to establish three partial structures as shown in Figure 1. In the HMBC spectrum, the long-range ^{1}H/^{13}C correlations observed from the isopropyl protons (δ 1.12, 6H, s) to the oxycarbons at δ 75.8 and 83.2 and from the methoxy protons (δ 3.20, 3H, s) to the latter

* To whom correspondence should be addressed. Tel: 886-7-5252000, ext. 5030. Fax: 886-7-5255020. E-mail: sheu@mail.nsysu.edu.tw.
† Department of Marine Biotechnology and Resources, National Sun Yat-sen University.
‡ Mansoura University.
§ Graduate Institute of Natural Products, Kaohsiung Medical University.
∥ Faculty of Biotechnology, Kaohsiung Medical University.
⊥ Asia-Pacific Ocean Research Center, National Sun Yat-sen University.

10.1021/np7007335 CCC: $40.75
Published on Web 05/01/2008

Table 1. ^{1}H NMR Data for Grandilobatins **1**−**5**

H#	**1**[a]	**2**[b]	**3**[b]	**4**[b]	**5**[a]
2	5.68 s	5.29 d (7.5)	5.35 d (10.0)	6.30 d (11.0)	6.25 d (10.7)
3	5.68 s	3.34 d (7.5)	3.08 dq (10.0, 6.5)	5.80 d (11.0)	5.63 d (10.7)
5α	1.73 m	2.04 dd (13.0, 5.0)	2.38 m	2.15 m	1.99 m
5*β*	1.73 m	1.48 m	2.48 br dd (10.0, 10.0)	2.07 m	2.07 m
6α	2.17 m	2.18 m	2.31 m 2.	2.19 m	1.71 m
6*β*	2.28 m	2.10 m	2.41 m	1.75 m	1.71 m
7	5.17 br dd (7.0,7.0)[c]	5.31 dd (7.0, 7.0)	5.37 br dd (6.5, 6.5)	5.23 br dd (8.0, 7.5)	2.28 m 2.89 quintet (8.8)
9α	2.97 d (15.0)	3.02 d (12.0)	3.04 d (12.0) 3.04	3.01 s	6.14 s
9*β*	3.18 d (15.0)	2.98 d (12.0)	2.90 d (12.0)	3.01 s	
11α	2.23 m	2.68 dd (16.5, 8.5)	2.61 dd (16.5, 10.0)	2.64 dd (15.0, 8.0)	2.05 m
11*β*	2.32 m	2.18 dd (16.5, 3.0)	2.22 dd (16.5, 4.0)	2.11 m	2.49 m
12	2.17 m	2.23 m	2.12 m	2.07 m	1.97 m
13α	1.25 m	1.59 m	1.33 m	1.43 m	1.41 m
13*β*	1.41 m	1.30 m	1.22 m	1.37 m	1.17 m
14α	1.42 m	2.06 m	2.09 ddd (13.0, 13.0, 5.0)	2.19 m	2.21 m
14*β*	1.74 m	1.93 ddd (13.0, 13.0, 4.0)	1.95 ddd (13.0, 13.0, 5.0)	2.17 m	2.01 m
16	1.12 3H, s	1.33 3H, s	1.33 3H, s	1.35 3H, s	1.33 3H, s
17	1.12 3H, s	1.34 3H, s	1.33 3H, s	1.35 3H, s	1.33 3H, s
18	1.39 3H, s	1.27 3H, s	1.14 3H, d (6.5)	1.74 3H, s	1.71 3H, s
19	1.78 3H, s	1.70 3H, s	1.76 3H, s	1.68 3H, s	1.88 3H, s
20	0.99 3H, d (7.0)	0.99 3H, d (7.0)	1.00 3H, d (6.5)	0.97 3H, d (6.5)	1.01 3H, d (6.3)
OMe	3.20 3H, s				

[a] Spectra recorded at 300 MHz. [b] 500 MHz in $CDCl_3$ at 25 °C. [c] The *J* values are in Hz in parentheses.

Table 2. ^{13}C NMR Data for Grandilobatins **1**−**5**

C#	**1**[a]	**2**[a]	**3**[b]	**4**[a]	**5**[a]
1	83.2 (qC)[c]	152.5 (qC)	147.9 (qC)	146.5 (qC)	147.0 (qC)
2	128.1 (CH)	119.7 (CH)	122.6 (CH)	118.7 (CH)	118.0 (CH)
3	140.8 (CH)	59.0 (CH)	47.8 (CH)	121.8 (CH)	121.9 (CH)
4	73.6 (qC)	61.9 (qC)	213.2 (qC)	136.7 (qC)	136.8 (qC)
5	43.8 (CH_2)	37.5 (CH_2)	39.5 (CH_2)	39.0 (CH_2)	38.0 (CH_2)
6	23.4 (CH_2)	23.1 (CH_2)	24.4 (CH_2)	25.4 (CH_2)	22.1 (CH_2)
7	129.1 (CH)	129.7 (CH)	127.6 (CH)	128.9 (CH)	29.8 (CH_2)
8	130.4 (qC)	130.0 (qC)	130.5 (qC)	129.2 (qC)	156.4 (qC)
9	52.3 (CH_2)	53.1 (CH_2)	52.9 (CH_2)	53.2 (CH_2)	126.8 (CH)
10	208.5 (qC)	208.5 (qC)	208.2 (qC)	209.8 (qC)	202.1 (qC)
11	51.5 (CH_2)	49.2 (CH_2)	49.6 (CH_2)	49.9 (CH_2)	52.4 (CH_2)
12	32.0 (CH)	28.3 (CH)	29.0 (CH)	29.1 (CH)	31.9 (CH)
13	31.5 (CH_2)	38.0 (CH_2)	35.8 (CH_2)	37.4 (CH_2)	37.1 (CH_2)
14	29.9 (CH_2)	25.9 (CH_2)	24.1 (CH_2)	25.0 (CH_2)	26.0 (CH_2)
15	75.8 (qC)	73.8 (qC)	73.7 (qC)	73.9 (qC)	73.9 (qC)
16	24.9 (CH_3)	29.6 (CH_3)	29.2 (CH_3)	29.7 (CH_3)	29.1 (CH_3)
17	26.3 (CH_3)	29.8 (CH_3)	29.4 (CH_3)	29.8 (CH_3)	29.3 (CH_3)
18	29.0 (CH_3)	18.0 (CH_3)	16.8 (CH_3)	17.1 (CH_3)	16.5 (CH_3)
19	18.1 (CH_3)	17.0 (CH_3)	17.8 (CH_3)	17.2 (CH_3)	22.9 (CH_3)
20	21.9 (CH_3)	21.4 (CH_3)	19.4 (CH_3)	20.3 (CH_3)	20.3 (CH_3)
OMe	51.5 (CH_3)				

[a] Spectra recorded at 75 MHz. [b] 125 MHz in $CDCl_3$ at 25 °C. [c] Attached protons were determined by DEPT experiments. The values are in ppm downfield from TMS.

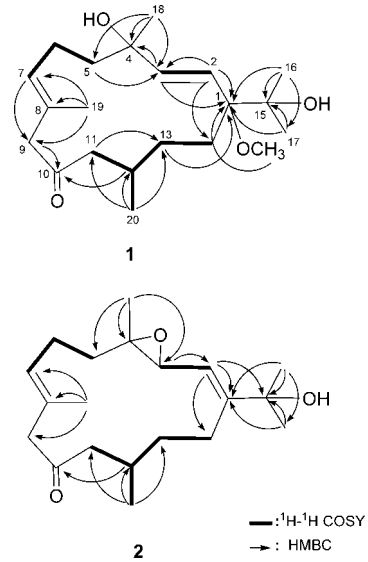

Figure 1. ^{1}H−^{1}H COSY and HMBC correlations for **1** and **2**.

oxycarbon positioned a hydroxyl and a methoxyl at C-15 and C-1, respectively. The second hydroxy group was positioned at C-4 by the HMBC correlations observed from H_3-18 (*δ* 1.39, 3H, s) to C-3 (*δ* 140.8, CH), C-5 (*δ* 43.8, CH_2), and an oxycarbon (*δ* 73.6, qC). Moreover, the correlations displayed from the olefinic methyl protons (*δ* 1.78, 3H, s) to C-9 (52.3, CH_2) and from H_2-9 (*δ* 2.97 and 3.18, each 1H, d, $J = 15.0$ Hz) to the carbonyl carbon at *δ* 208.5 located the carbonyl oxygen at C-10. On the basis of above findings and other detailed HMBC correlations (Figure 1), the planar structure of oxocembranoid **1** was established.

The relative stereochemistry of **1** was determined by analysis of the NOESY spectrum of **1**, measured in C_6D_6 (Figure 2). Assuming the *β*-orientation of the hydroxyisopropyl group at C-1, it was found that the α-oriented methoxy protons (*δ* 3.06, s) exhibited a strong NOE correlation with one of H_2-14 (*δ* 1.42, m). Therefore, this C-14-associated proton was assigned as H-14α. The other proton attached at C-14 (*δ* 1.78, m) was then assigned as H-14*β*. The strong NOE interaction of H-3 (*δ* 5.64, d, $J = 16.5$ Hz) with H-14*β*, but not with H-2 (*δ* 5.76, d, $J = 16.5$ Hz), reflected the upward orientation of H-3 and the downward orientation of H-2. This finding together with the large *J* values of both H-2 and H-3 indicated the *E* geometry of the double bond at C-2/C-3. Moreover, the NOE interactions shown between the downward proton H-2 and both H_3C−O and H_3-18, and between H_3-18 and H-3, implied the α-orientation of the methyl group at C-4. The NOE correlations of H-3 with H-7, H-7 with H-9*β* (*δ* 2.89, d, $J = 14.5$ Hz), and H-9*β* with H-12 (*δ* 2.03, m) indicated the upward position of H-7, and thus the *β*-orientation of H-12 and α-orientation of the secondary methyl at C-12. This was further supported by the NOE interaction of H-14*β* with H-12. The NOE correlation of H_3-19 with H_2-6 and the chemical shift value of C-19 (18.3 ppm) reflected the *E* geometry of the trisubstituted double bond at C-7 and C-8 in the molecule. On the basis of the above findings and other detailed NOE correlations (Figure 2), the structure of grandilobatin A (**1**) was fully established as (1*R**,4*R**,12*S**,2*E*,7*E*)-1-methoxy-4,15-dihydroxycembra-2,7-dien-10-one.

Grandilobatin B (**2**) was found to possess the molecular formula $C_{20}H_{32}O_3$ as revealed by the HRESIMS spectrum (*m*/*z* 343.2250 $[M + Na]^+$) and NMR data (Tables 1 and 2). The IR absorption band at 3434 cm^{-1} and the ion peak appearing in the EIMS at *m*/*z*

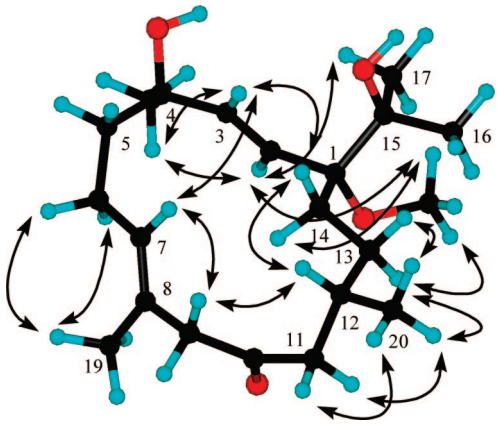

Figure 2. Computer-generated model for **1** using MM2 force field calculations and key NOE correlations.

302 $[M - H_2O]^+$ indicated the presence of one hydroxy group in **2**. The IR absorptions at 1707 and 1660 cm^{-1} also revealed ketone and olefinic functionalities in the molecule. This was supported by the presence of five carbon signals at δ 208.5 (qC), 152.5 (qC), 130.0 (qC), 129.7 (CH), and 119.7 (CH) and the two proton signals at δ 5.29 (1H, d, J = 7.5 Hz) and δ 5.31 (1H, dd, J = 7.0, 7.0 Hz), which are attributable to one carbonyl group and two trisubstituted double bonds. Moreover, a trisubstituted epoxide was found from the NMR signals at δ_C 61.9 (qC), 59.0 (CH) and δ_H 3.34 (1H, d, J = 7.5 Hz). Compound **2** displayed signals of five methyls, including one olefinic methyl (δ 1.70, s), three methyls attached to oxycarbons (δ 1.34, 1.33, and 1.27 each s), and a secondary methyl (δ 0.99, d, J = 7.0 Hz). From these findings, combined with the NMR spectral comparison with **1**, metabolite **2** was suggested to be another oxocembranoid possessing one epoxide, one hydroxy group, and two olefinic bonds. The close similarities of the carbon signals of C-5 to C-14, C-19, and C-20 indicated the presence of an analogous partial structure with that of **1**. Moreover, the HMBC correlations displayed from H_3-18 to the epoxide carbons C-4 (δ 61.9, qC) and C-3 (δ 59.0, CH) coupled with the $^1H-^1H$ COSY correlation found between the epoxide proton (δ 3.34 d, J = 7.5 Hz) and the olefinic proton at δ 5.29 (d, J = 7.5 Hz) implied the C-3/C-4 and C-1/C-2 positions of the epoxy group and a trisubstituted double bond, respectively. Further investigations on the $^1H-^1H$ COSY and HMBC correlations (Figure 1) positioned the second trisubstituted double bond and the ketone group at C-7/C-8 and C-10, respectively, and hence established the gross structure of **2**.

The relative stereochemistry of **2** was resolved on the basis of comparison of NMR data with those of related compounds and analysis of NOE correlations (Figure 3). It was found that the chemical shifts and J values for H-2 (δ 5.16, d, J = 8.0 Hz) and H-3 (δ 3.44, d, J = 8.0 Hz) of a known 3,4-epoxycembranoid (**6a**)[13] are very similar to those of **2**. Also, the chemical shifts of C-3 (δ 59.3, CH) and C-4 (δ 62.0)[13] of **6b** resembled those of **2**. Thus, the α-orientation of the epoxide was assumed. From NOE correlations between the epoxide proton H-3 (δ 3.34, d, J = 7.5 Hz) and both H-14β (δ 1.93, ddd, J = 13.0, 13.0, 4.0 Hz) and H-13β (δ 1.30, m) and between H_3-20 (δ 0.99, 3H, d, J = 7.0 Hz) and H-13α (δ 1.59, m), H-14α (δ 2.06, m), and H-14β (δ 1.93, ddd, J = 13.0, 13.0, 4.0 Hz), it was possible to determine the α-orientation of the methyl group at C-12, as shown in Figure 3. Moreover, it was found that H-2 (δ 5.29, d, J = 7.5 Hz) exhibited a NOE interaction with the hydroxyisopropyl protons and H_3-18 (δ 1.27, s), disclosing the *E* geometry of the 1,2-double bond. The *E* geometry of the 7,8-double bond was also revealed from the NOE interactions displayed by H_3-19 with H_2-6 and the chemical shift of C-19 (δ 17.0). On the basis of the above findings and other detailed NOE correlations

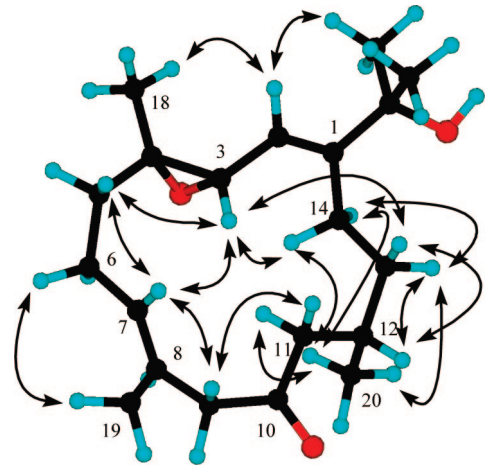

Figure 3. Computer-generated model for **2** using MM2 force field calculations and key NOE correlations.

(Figure 3), the structure of grandilobatin B (**2**) was deduced as (3*S**,4*S**,12*S**,1*E*,7*E*)-3,4-epoxy-15-hydroxycembra-1,7-dien-10-one.

Grandilobatin C (**3**) exhibited the pseudomolecular ion peak at *m*/*z* 343.2251 $[M + Na]^+$ in the HRESIMS, suggesting the molecular formula $C_{20}H_{32}O_3$ and five degrees of unsaturation. The IR absorption at 3422 cm^{-1} and the EIMS ion peak at *m*/*z* 302 $[M - H_2O]^+$ indicated the presence of one hydroxy group in **3**. Two ketocarbonyl groups were found from the IR (ν_{max} 1701 cm^-) and ^{13}C NMR (δ 208.2 and 213.2, each qC) spectral data of **3**. The signals appearing at δ_H 5.35 (1H, d, J = 10.0 Hz) and 5.37 (1H, dd, J = 6.5, 6.5 Hz) and δ_C 122.6 (CH), 127.6 (CH), 130.5 (qC), and 147.9 (qC) were attributable to two trisubstituted double bonds. Comparison of the NMR data of **3** with those of **2** (Table 2) revealed that the trisubstituted epoxide signals in 2 (δ_H 3.34; δ_C 59.0, CH and 61.9, qC) were replaced by signals of a carbonyl group (δ_C 213.2, qC), a methine (δ_H 3.08,1H, dq, J = 10.0, 6.5 Hz; δ_C 47.8, CH), and a secondary methyl group (δ_H 1.14, 3H, d, J = 6.5 Hz; δ_C 16.8, CH_3). The above methine proton was found to be $^1H-^1H$ COSY correlated (Figure 4) with both the above-mentioned secondary methyl protons and the olefinic proton at C-2 (δ 5.35, d, J = 10.0 Hz), assigning the C-3 location of this secondary methyl group (H_3-18). Furthermore, the HMBC correlations from H_3-18 to C-2 (δ 122.6, CH), C-3 (δ 47.8, CH), and a carbonyl carbon (δ 213.2) indicated the C-4 position of one of the two carbonyl groups. Moreover, the similar chemical shifts for carbons C-6 to C-14 of **3** with those of **2** together with detailed $^1H-^1H$ COSY and HMBC correlations for **3** (Figure 4) indicated that the second carbonyl group and the other olefinic bond should be positioned at C-10 and C-7/C-8, respectively. On the basis of the above findings, **3** was found to be a novel C-3 methylated isocembranoid with a planar structure, as shown in Figure 4.

The *E* geometry of the two trisubstituted double bonds at C-1/C-2 and C-7/C-8 in **3** was assigned from the NOE interactions of H-2 (δ 5.35, d, J = 10.0 Hz) with the protons of the hydroxyisopropyl methyls (δ 1.33, 6H, s) and of H_3-19 (δ 1.76, 3H, s) with H-6 (δ 2.31, m), respectively. Assuming the α-orientation of the methyl substituent at C-12, the strong NOE correlations displayed by H_3-20 (δ 1.00, 3H, d, J = 6.5 Hz) with H_2-11 and H_2-14 indicated the downward orientations of all the methylene groups at both C-11 and C-14, as illustrated by a molecular model (Figure 5). Moreover, the NOE interactions displayed by H-11α (δ 2.61, dd, J = 16.5, 10.0 Hz) with H-9α (δ 3.04, d, J = 12.0 Hz), H-9α with H-7 (δ 5.37, br dd, J = 6.5, 6.5), and one of the downward-oriented H-14 (δ 1.95, ddd, J = 13.0, 13.0, 5.0 Hz) with H-3 revealed the downward orientations of H-7 and H-3. The α-orientation of H-3 was also confirmed by NOE correlations between H-3

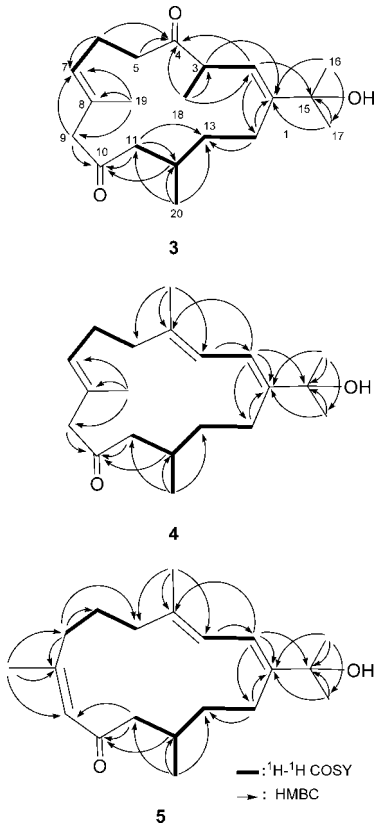

Figure 4. ^{1}H−^{1}H COSY and HMBC correlations for **3**−**5**.

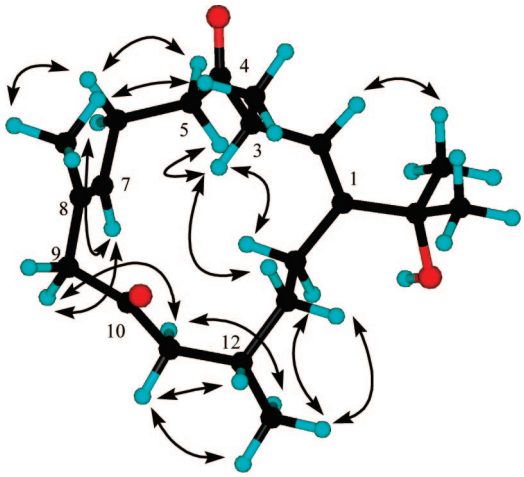

Figure 5. Computer-generated model for **3** using MM2 force field calculations and key NOE correlations.

and H-13α. Therefore, the NOE response exhibited between H_3-18 and H_3-19 assigned the β-orientation of the methyl group at C-3, and hence the *R** configuration at C-3. This result, together with other detailed NOE correlations of **3** (Figure 5), established the structure of grandilobatin C as shown in formula **3**. Metabolite **3** possesses a novel skeleton formed by the methyl group at C-4 of **2** rearranging to C-3 by acid-catalyzed ring-opening of the 3,4-epoxide and the following methyl shift.

Grandilobatin D (**4**) was found to possess the molecular formula $C_{20}H_{32}O_2$ as revealed by the HRESIMS (*m*/*z* 327.2303 [M + Na]$^+$) and NMR data (Tables 1 and 2). The IR spectrum suggested the presence of hydroxy, carbonyl, and olefinic moieties in **4** (ν_{max} 3443, 1707, and 1667 cm^{-1}, respectively). The ^{13}C NMR spectral data of **4** were found to be very similar to those of **2**, except for the replacement of the two carbon signals of the epoxide moiety in **2** by the signals of a trisubstituted double bond in **4** (δ 121.8, CH, C-3 and 136.7, qC, C-4). This double bond was positioned at C-3/C-4 due to the ^{1}H−^{1}H COSY correlation found between the *trans*-oriented H-2 (δ 6.30, d, J = 11.0 Hz) and H-3 (δ 5.80, d, J = 11.0 Hz) and the HMBC correlations observed from the olefinic methyl protons at δ 1.74 (3H, s) to C-3 and C-4 and from H-2 to C-1, C-4, and C-15 (Figure 4). Furthermore, the *E* geometry of the 3,4-double bond was deduced from the NOE correlation of H_3-18 with H-2 and not with H-3. Thus, **4** was identified as (12*S**,1*E*,3*E*,7*E*)-15-hydroxycembra-1,3,7-trien-10-one.

The related metabolite, grandilobatin E (**5**), possessed the same molecular formula as **4**, as indicated by the HRESIMS (*m*/*z* 327.2300, [M + Na]$^+$) and NMR data (Tables 1 and 2). It was found that **5** possesses an α,β-unsaturated ketone moiety, as interpreted from the IR spectrum (ν_{max} 1680 cm^{-1}) and NMR data (δ_H 6.14, 1H, s; and δ_C 202.1, qC, 156.4, qC and 126.8, CH). Also, the ^{1}H−^{1}H COSY correlations from H_2-5 to H_2-6 and then to H_2-7 suggested the isomerization of the 7,8-double bond in **4** to the 8,9-double bond in **5**. This was further supported by the HMBC correlations observed from H-20 (δ 1.01, 3H, d, J = 6.3 Hz) to C-11 (δ 52.4, CH), from H_2-11 (δ 2.05, m and 2.49, m) to the carbonyl carbon C-10 (δ 202.1, qC) and the olefinic carbon C-9 (δ 126.8, CH), and from H_3-19 (δ 1.88, 3H, s) to the olefinic carbons C-8 (δ 156.4, qC) and C-9. Moreover, the NOESY spectrum of **5** showed a strong NOE interaction for the olefinic methyl group at C-8 with H-9. Thus, the *Z* geometry of the trisubstituted double bond at C-8/C-9 was assigned. On the basis of the above results, the structure of grandilobatin E (**5**) was established as (12*S**,1*E*,3*E*,8*Z*)-15-hydroxycembra-1,3,8-trien-10-one.

The cytotoxicity of the diterpenoids **1**−**5** against the growth of liver (Hep G2), breast (MCF-7 and MDA-MB-23), and lung (A-549) carcinoma cells was studied. It was found that only **4** exhibited weak cytotoxicity (IC_{50} 15.8 μg/mL) against MDA-MB-23 cells; the other compounds were inactive toward the above cancer cells.

The *in vitro* anti-inflammatory effect of diterpenoids **2** and **4** was also tested, as they were obtained in larger quantifies than the other metabolites. In this assay, the accumulation of pro-inflammatory iNOS and COX-2 proteins in LPS-stimulated RAW 264.7 macrophage cells was evaluated using immunoblot analysis. It was found that at 50 μM compound **4** reduced the levels of iNOS to 28.7 ± 4.2% relative to the control cells stimulated with LPS alone, while it was inactive toward the expression of COX-2 protein. However, the same concentration of the 3,4-epoxy derivative **2** did not produce any inhibition of LPS-induced iNOS and COX-2 expression (Figure 6), but instead increased the induction of iNOS and COX-2 protein to 112.4% and 117.3%, respectively, relative to those induced by LPS-stimulated RAW 264.7 macrophage cells.

Experimental Section

General Experimental Procedures. Optical rotations were measured on a Jasco DIP-1000 digital polarimeter. IR spectra were recorded on a Jasco FT-5300 infrared spectrophotometer. NMR spectra were recorded on a Bruker AVANCE-DPX 300 FT-NMR at 300 MHz for ^{1}H and 75 MHz for ^{13}C or on a Varian Unity INOVA 500 FT-NMR at 500 MHz for ^{1}H and 125 MHz for ^{13}C, respectively, in $CDCl_3$ or C_6D_6 using TMS as internal standard. Low-resolution MS data were obtained by EI on a VG Quattro GC/MS spectrometer or by ESI on a Bruker APEX II mass spectrometer. HRMS data were recorded by ESI FT-MS on a Bruker APEX II mass spectrometer. Si gel 60 (Merck, 230−400 mesh) and Sephadex LH-20 (Pharmacia) were used for open CC. Precoated Si plates (Merck, Kieselgel 60 F_{254}, 0.2 mm) were used for analytical TLC analyses. Isolation by HPLC was performed by a Shimadzu SPD-10A instrument equipped with a normal-phase column (Hibar Lichrosorb Si-60, 7 μm, 250 × 25 mm) or a reversed phase column (Hibar Purospher RP-18e, 5 μm, 250 × 10 mm).

Animal Material. The soft coral *S. grandilobata* was collected by hand using scuba off the coast of the southernmost tip of Pingtung County, Taiwan, in June 2004, at depths of 15 to 20 m and stored in a freezer until extraction. A voucher sample (SC-62) was deposited at

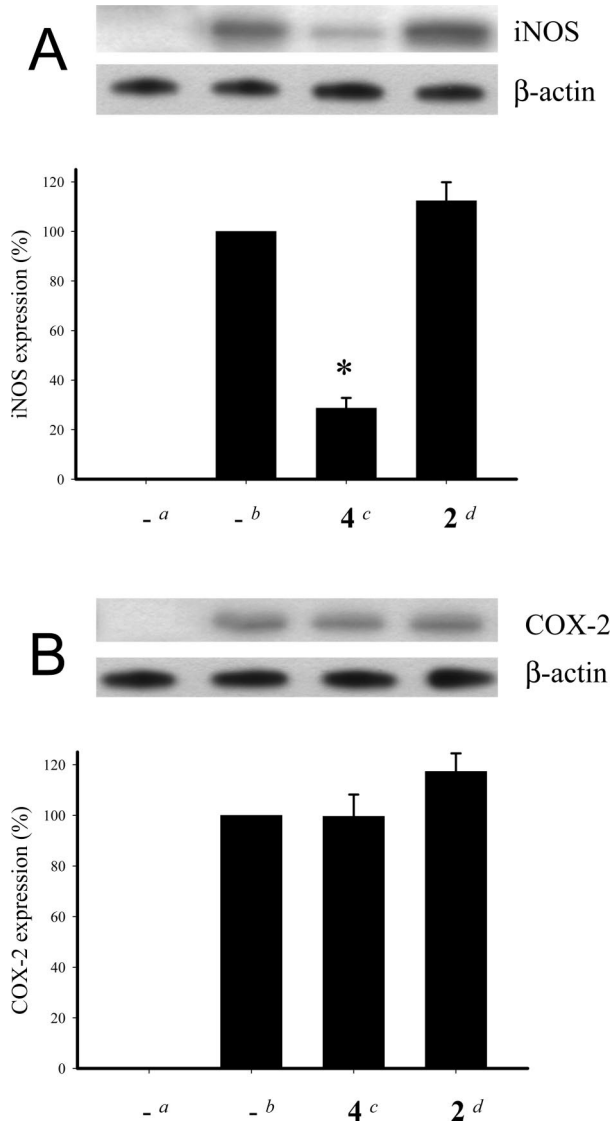

Figure 6. Effect of compounds **2** and **4** on iNOS and COX-2 protein expression of RAW264.7 macrophage cells by immunoblot analysis. (A) Immunoblots of iNOS and β-actin. (B) Immunoblots of COX-2 and β-actin. The values are mean ± SEM ($n = 6$). Relative intensity of the LPS alone stimulated group was taken as 100%. *Significantly different from LPS alone stimulated group (*$P < 0.05$). [a]Cells not stimulated, [b]stimulated with LPS, [c]stimulated with LPS in the presence of **4** (50 μM), [d]stimulated with LPS in the presence of **2** (50 μM).

the Department of Marine Biotechnology and Resources, National Sun Yat-sen University.

Extraction and Separation. The frozen bodies of *S. grandilobata* (0.9 kg, wet wt) were minced and extracted exhaustively with EtOH (1 L × 5). The EtOH extract was filtered and concentrated under reduced pressure. The residue was partitioned between CH_2Cl_2 and H_2O. The organic layers was concentrated, and the residue was chromatographed on Si gel by CC and eluted with EtOAc in *n*-hexane (0−100%, gradient) then with MeOH in EtOAc (5−50%, gradient) to yield 17 fractions. The eluted fractions were monitored by ^{1}H NMR spectroscopy, and fraction 7 (0.46 g), eluted by EtOAc−*n*-hexane (7:20), was selected for its terpenoidal content. Fraction 7 was separated by preparative normal-phase HPLC using acetone−EtOAc−*n*-hexane (1:1:25) to give 10 subfractions (7A−7J). Subfraction 7F was rechromatographed by normal-phase HPLC using acetone−*n*-hexane (1:30) to yield **4** (35.6 mg) and three subfractions, 7FB, 7FC, and 7FD, respectively. Subfraction 7FB was subjected to repeated chromatography by normal-phase HPLC using acetone−*n*-hexane (1:49) to give **2** (5.5 mg). Subfraction 7FC was purified by reversed-phase HPLC using acetone−H_2O (4:3) then followed by normal-phase HPLC using CH_2Cl_2−MeOH (99:1) to afford **3** (1.8 mg). Subfraction 7FD was purified by reversed-phase HPLC using MeOH−H_2O (3:1) followed by normal-phase HPLC using acetone−*n*-hexane (1:3) to give **1** (1.1 mg). Finally, subfraction 7I was purified by reversed-phase HPLC using MeOH−H_2O (3:1) to yield **5** (3.8 mg).

Grandilobatin A (1): colorless oil; $[\alpha]^{25}_D$ +18.2 (*c* 0.4, $CHCl_3$); IR (neat) ν_{max} 3422, 2956, 2926, 2866, 1699, 1653, 1521, 1375, and 1076 cm^{-1}; ^{1}H and ^{13}C NMR data ($CDCl_3$), see Tables 1 and 2, respectively; ^{1}H NMR (C_6D_6, 500 MHz) δ 5.76 (1H, d, $J = 16.5$ Hz, H-2), 5.64 (1H, d, $J = 16.5$ Hz, H-3), 5.05 (1H, dd, $J = 6.5$, 5.5 Hz, H-7), 3.06 (3H, s, OMe), 2.89 (1H, d, $J = 14.5$ Hz, H-9α), 2.59 (1H, d, $J = 14.5$ Hz, H-9β), 2.20 (1H, m, H-6α), 2.12 (1H, dd, $J = 14.0$, 9.0 Hz, H-11β), 2.03 (1H, m, H-12), 2.00 (1H, m, H-6β), 1.89 (1H, dd, $J = 14.0$, 3.0 Hz, H-11α), 1.78 (1H, m, H-14α), 1.75 (3H, s, H_3-19), 1.63 (1H, ddd, $J = 14.0$, 9.0, 3.0 Hz, H-5α), 1.54 (1H, ddd, $J = 14.0$, 9.0, 3.0 Hz, H-5β), 1.49 (1H, m, H-13α), 1.45 (1H, m, H-13β), 1.42 (1H, m, H-14β), 1.24 (3H, s, H_3-16), 1.25 (3H, s, H_3-17), 1.09 (3H, s, H_3-18), 0.83 (3H, d, $J = 6.5$ Hz, H_3-20); ^{13}C NMR (C_6D_6, 500 MHz) δ 208.6 (qC, C-10), 141.3 (CH, C-3), 130.9 (CH, C-7), 129.5 (CH, C-2), 83.8 (qC, C-1), 129.1 (qC, C-8), 76.0 (qC, C-15), 73.3 (qC, C-4), 52.3 (CH_2, C-9), 51.6 (CH_3, OMe), 51.5 (CH_2, C-11), 44.4 (CH_2, C-5), 32.2 (CH, C-12), 31.9 (CH_2, C-13), 29.5 (CH_2, C-14), 29.5 (CH_3, C-18), 26.9 (CH_3, C-17), 25.5 (CH_3, C-16), 23.8 (CH_2, C-6), 22.2 (CH_3, C-20), 18.3 (CH_3, C-19); ESIMS *m/z* 375 [100, $(M + Na)^+$]; HRESIMS *m/z* 375.2514 (calcd for $C_{21}H_{36}O_4Na$, 375.2511).

Grandilobatin B (2): colorless oil; $[\alpha]^{25}_D$ +103.2 (*c* 2.2, $CHCl_3$); IR (neat) ν_{max} 3434, 2959, 2929, 2870, 1707, 1660, 1456, 1383, and 1121 cm^{-1}; ^{1}H and ^{13}C NMR data ($CDCl_3$), see Tables 1 and 2, respectively; EIMS *m/z* 320 [0.5, $(M)^+$], 302 [1.1, $(M - H_2O)^+$], 287 (1.6), 259 (1.7), 229 (1.1), 219 (1.1), 177 (3.2), 166 (10.0), 151 (9.7), 137 (11.6), 123 (25.1), 107 (27.8), and 95 (33.1); HRESIMS *m/z* 343.2250 (calcd for $C_{20}H_{32}O_3Na$, 343.2249).

Grandilobatin C (3): colorless oil; $[\alpha]^{25}_D$ −13.9 (*c* 0.7, $CHCl_3$); IR (neat) ν_{max} 3422, 2956, 2926, 2876, 1701, 1653, 1458, 1397, and 1113 cm^{-1}; ^{1}H and ^{13}C NMR data ($CDCl_3$), see Tables 1 and 2, respectively; EIMS *m/z* 320 [0.6, $(M)^+$], 302 [0.8, $(M - H_2O)^+$], 285 (2.5), 267 (9.8), 257 (2.6), 239 (6.5), 229 (4.9), 167 (5.1), 149 (9.8), 133 (18.4), 121 (9.5), 112 (12.0), 109 (13.8), and 98 (39.9); ESIMS *m/z* 359 [5, $(M + K)^+$] and 343 [100, $(M + Na)^+$]; HRESIMS *m/z* 343.2251 (calcd for $C_{20}H_{32}O_3Na$, 343.2249).

Grandilobatin D (4): colorless oil; $[\alpha]^{25}_D$ +223.0 (*c* 1.0, $CHCl_3$); IR (neat) ν_{max} 3443, 2969, 2932, 2872, 1707, 1667, 1454, 1370, 1181, and 1146 cm^{-1};^{1}H and ^{13}C NMR data in $CDCl_3$, see Tables 1 and 2, respectively; ESIMS *m/z* 327 [100, $(M + Na)^+$]; HRESIMS *m/z* 327.2303 (calcd for $C_{20}H_{32}O_2Na$, 327.2300).

Grandilobatin E (5): colorless oil; $[\alpha]^{25}_D$ −67.8 (*c* 1.5, $CHCl_3$); IR (neat) ν_{max} 3430, 2960, 2926, 1680, 1640, 1614, 1458, 1377, and 1146 cm^{-1}; ^{1}H and ^{13}C NMR data in $CDCl_3$, see Tables 1 and 2, respectively; ESIMS *m/z* 343 [50, $(M + K)^+$] and 327 [50, $(M + Na)^+$]; HRESIMS *m/z* 327.2300 (calcd for $C_{20}H_{32}O_2Na$, 327.2300).

***In Vitro* Anti-inflammatory Assay.** The anti-inflammatory assay was modified from Ho et al.[14] and Park et al.[15] Murine RAW 264.7 macrophages were obtained from the American Type Culture Collection (ATCC, No TIB-71) and cultured in Dulbecco's modified essential medium (DMEM) containing 10% heat-inactivated fetal bovine serum, at 37 °C in a humidified 5% CO_2−95% air incubator under standard conditions. Inflammation in macrophages was induced by incubating them for 16 h in a medium containing only LPS (0.01 μg/mL; Sigma) without the presence of test compounds. For the anti-inflammatory activity assay, compounds **2** and **4** were added to the cells 5 min before LPS challenge, respectively. Then, cells were washed with ice-cold PBS and lysed in ice cold lysis buffer, then centrifuged at 20000*g* for 30 min at 4 °C. The supernatant was decanted from the pellet and retained for Western Blot analysis. Protein concentrations were determined by the DC protein assay kit (Bio-Rad) modified by the method of Lowry et al.[16] Samples containing equal quantities of proteins were subjected to SDS-polyacrylamide gel electrophoresis, and the separated proteins were electrophoretically transferred to polyvinylidene difluoride membranes (PVDF; Immobilon-P, Millipore, 0.45 μM pore size). The PVDF membranes were incubated for 180 min at room temperature with antibody against inducible nitric oxide synthase (iNOS; 1:1000 dilution; Transduction Laboratories) and cyclooxygenase-2 (COX-2; 1:1000 dilution; Cayman Chemical) protein. The blots were detected using ECL detection reagents (Perkin-Elmer, Western Blot

chemiluminescence reagent plus) according to the manufacturer's instructions and finally exposed to X-ray film (Kodak X-OMAT LS, Kodak). The membranes were reprobed with a monoclonal mouse anti-β-actin antibody (1:2500, Sigma) as the loading control. After X-ray film scanning, the integrated optical density of the bands was estimated (Image-Pro plus 4.5 software) and normalized to the background values. Relative variations between the bands of the drug-treated samples and the samples treated with LPS alone were calculated in the same image.

Cytotoxicity Testing. Cell lines were purchased from the American Type Culture Collection (ATCC). Cytotoxicity assays of the test compounds **1**−**5** were performed using the MTT [3-(4,5-dimethylthiazol-2-yl)-2,5-diphenyltetrazolium bromide] colorimetric method.[17,18]

Acknowledgment. This work was supported by grants from the Ministry of Education (96C031702) and National Science Council of Taiwan (Contract No. 95-2113-M-110-011-MY3) awarded to J.-H.S.

Supporting Information Available: This material is available free of charge via the Internet at http://pubs.acs.org.

References and Notes

(1) Blunt, J. W.; Copp, B. R.; Hu, W.-P.; Munro, M. H. G.; Northcote, P. T.; Prinsep, M. R. *Nat. Prod. Rep* **2007**, *24*, 31–86.
(2) Su, J.-H.; Ahmed, A. F.; Sung, P.-J.; Chao, C.-H.; Kuo, Y.-H.; Sheu, J.-H. *J. Nat. Prod.* **2006**, *69*, 1134–1139.
(3) Sheu, J.-H.; Chang, K.-C.; Sung, P.-J.; Duh, C.-Y.; Shen, Y.-C. *J. Chin. Chem. Soc.* **1999**, *46*, 253–257.
(4) Duh, C.-Y.; Wang, S.-K.; Tseng, H.-K.; Sheu, J.-H.; Chiang, M. Y. *J. Nat. Prod.* **1998**, *61*, 844–847.
(5) Hou, R.-S.; Duh, C.-Y.; Chang, M. Y.; Lin, C.-N. *J. Nat. Prod.* **1995**, *58*, 1126–1130.
(6) Duh, C.-Y.; Hou, R.-S. *J. Nat. Prod.* **1996**, *59*, 595–598.
(7) Tseng, Y.-J.; Ahmed, A. F.; Dai, C.-F.; Chiang, M. Y.; Sheu, J.-H. *Org. Lett.* **2005**, *7*, 3813–3816.
(8) Ahmed, A. F.; Su, J.-H.; Kuo, Y.-H.; Sheu, J.-H. *J. Nat. Prod.* **2004**, *67*, 2079–2082.
(9) Ahmed, A. F.; Shiue, R.-T.; Wang, G.-H.; Dai, C.-F.; Kuo, Y.-H.; Sheu, J.-H. *Tetrahedron* **2003**, *59*, 7337–7344.
(10) Sheu, J.-H.; Ahmed, A. F.; Shiue, R.-T.; Dai, C.-F.; Kuo, Y.-H. *J. Nat. Prod.* **2002**, *65*, 1904–1908.
(11) Tseng, Y.-J.; Ahmed, A. F.; Hsu, C.-H.; Su, J.-H.; Dai, C.-F.; Sheu, J.-H. *J. Chin. Chem. Soc.* **2007**, *54*, 1041–1044.
(12) Ahmed, A. F.; Tai, S.-H.; Wu, Y.-C.; Sheu, J.-H. *Steroids* **2007**, *72*, 368–374.
(13) Kobayashi, M.; Osabe, K. *Chem. Pharm. Bull.* **1989**, *37*, 1192–1196.
(14) Ho, F.-M.; Lai, C.-C.; Huang, L.-J.; Kuo, T.-C.; Chao, C.-M.; Lin, W.-W. *Br. J. Pharmacol.* **2004**, *141*, 1037–1047.
(15) Park, E.-K.; Shin, Y.-W.; Lee, H.-U.; Kim, S.-S.; Lee, Y.-C.; Lee, B.-Y.; Kim, D.-H. *Biol. Pharm. Bull.* **2005**, *28*, 652–656.
(16) Lowry, D. H.; Rosebrough, N. J.; Farr, A. L.; Randall, R. J. *J. Biol. Chem.* **1951**, *193*, 265–275.
(17) Alley, M. C.; Scudiero, D. A.; Monks, A.; Hursey, M. L.; Czerwinski, M. J.; Fine, D. L.; Abbott, B. J.; Mayo, J. G.; Shoemaker, R. H.; Boyd, M. R. *Cancer Res.* **1988**, *48*, 589–601.
(18) Scudiero, D. A.; Shoemaker, R. H.; Paull, K. D.; Monks, A.; Tierney, S.; Nofziger, T. H.; Currens, M. J.; Seniff, D.; Boyd, M. R. *Cancer Res.* **1988**, *48*, 4827–4833.

NP7007335